Comparison of quantal, classical, and semiclassical behavior at an isolated avoided crossing

D. W. Noid, M. L. Koszykowski, and R. A. Marcus

Citation: The Journal of Chemical Physics **78**, 4018 (1983); doi: 10.1063/1.445127
View online: http://dx.doi.org/10.1063/1.445127
View Table of Contents: http://scitation.aip.org/content/aip/journal/jcp/78/6?ver=pdfcov
Published by the AIP Publishing

Comparison of quantal, classical, and semiclassical behavior at an isolated avoided crossing

D. W. Noid

Oak Ridge National Laboratory, Oak Ridge, Tennessee 37830
and Department of Chemistry, Univeristy of Tennessee, Knoxville, Tennessee 37916

M. L. Koszykowski

Sandia National Laboratory, Livermore, California 94550

R. A. Marcus[a)]

Arthur Amos Noyes Laboratory of Chemical Physics, California Institute of Technology, Pasadena, California 91125
(Received 8 September 1982; accepted 21 October 1982)

The quantal and classical/semiclassical behavior at an isloated avoided crossing are compared. While the quantum mechanical eigenvalue perturbation parameter plots exhibit the avoided crossing, the corresponding primitive semiclassical eigenvalue plots pass through the intersection. Otherwise, the eigenvalues agree well with the quantum mechanical values. The semiclassical splitting at the intersection is calculated from an appropriate Fourier transform. In the quasiperiodic regime, a quantum state near an avoided crossing is seen to exhibit typically more delocalization than the classical state. However, trajectories near the "separatrix" display a quasiperiodic "transition" between two zeroth order classical states.

INTRODUCTION

Bill Flygare was a colleague of one of ours for many years, one whose stimulating and joyous presence we shall always remember. His interests being mainly spectroscopic and ours largely in kinetics or collision dynamics, they occasionally overlapped. One overlap in which we belived he would have been interested involves avoided crossings, the subject of the present paper and one which plays a role in intramolecular energy transfer.

If one plots two vibrational energy eigenvalues of a molecule vs a perturbation parameter the curves may intersect or, if the two states are suitably coupled by the perturbation, undergo an avoided crossing. Such avoided crossings can produce local changes in a spectrum, on one hand, and offer a way of substantially mixing nodal patterns of the two states, on the other. If a particular state participates simultaneously in many (i.e., "overlapping") avoided crossings, it takes on a statistical behavior which is expected to expedite energy redistribution in a wave packet for an isolated molecule, and should generate, as well, an irregular spectrum.[1-3] In the present paper we compare classical/semiclassical and quantum behavior for an isolated avoided crossing.

THEORY AND RESULTS

We have noted elsewhere that at an avoided crossing of two levels of E_1 and E_2 the angular frequency $(E_1 - E_2)/\hbar$ becomes small (equals zero for the diabatic states), and correspondingly in the classical behavior one expects that some frequency of the motion will approach zero.[1-3] Such a motion corresponds to a nearly periodic trajectory, which is associated with a classical resonance. To study the behavior at an isolated avoided crossing we consider the following Hamiltonian,

$$H = \tfrac{1}{2}(p_x^2 + p_y^2 + \omega_x^{02}x^2 + \omega_y^{02}y^2) - ax^3 - ay^3 + \lambda x^2y^2 - bxy^3 , \quad (1)$$

with $\omega_x^0 = 3\omega_y^0 = 3$. Without the x^3 and y^3 terms the two eigenvalues vs λ plots considered below would intersect only at $\lambda = 0$. The λx^2y^2 term produces eigenvalues vs λ plots of different slopes. Because of the commensurability of ω_x^0 and ω_y^0 and the smallness of the perturbation ($a = 0.02$, $b = 0.005$ to 0.03, and λ varied from 0 to approximately 0.1) a nearly exact 3:1 classical resonance occurs as some λ in this range. At this λ and at nearby λ's, one expects a strong distortion of the classical motion. Its influence on the quantum and semiclassical behavior is described below.

Quantum calculation

The quantum mechanical eigenvalues were calculated and the avoided crossing of the ($n_x = 0$, $n_y = 3$) and the ($n_x = 1$, $n_y = 0$) states was studied. These states are nearly degenerate. The calculation was made using a 100-element basis set of harmonic oscillator states (10 each for ψ_x and for ψ_y), using an EISPAC matrix diagonalization package.[4] The states studied are the fourth and fifth. Their eigenvalues are accurate to 0.0001, as judged by use of a larger basis set.

For $b = 0.005$ the eigenvalues were determined in λ increments of 0.01 (0 to 0.1), except near the avoided crossing, where $\Delta\lambda$ was 0.005. For $b = 0.01$ and 0.03, the λ increments were 0.01. Plots of these (0, 3) and (1, 0) eigenvalues vs λ are given in Figs. 1–3. (Units of $\hbar = 1$ are used throughout the paper.) Two wave functions for a λ far removed from the λ at the avoided crossing are plotted in Fig. 4, while those for

[a)]Contribution No. 6729.

 0021-9606/83/064018-07$2.10

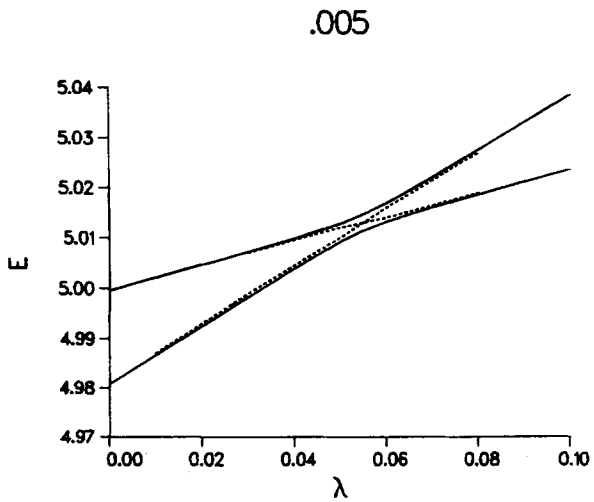

FIG. 1. Plot of quantum mechanical eigenvalues vs perturbation parameter λ for the fourth and fifth eigenvalues of the Hamiltonian (1), with $b = 0.005$. Semiclassical eigenvalues of Table II are indicated with a dotted line.

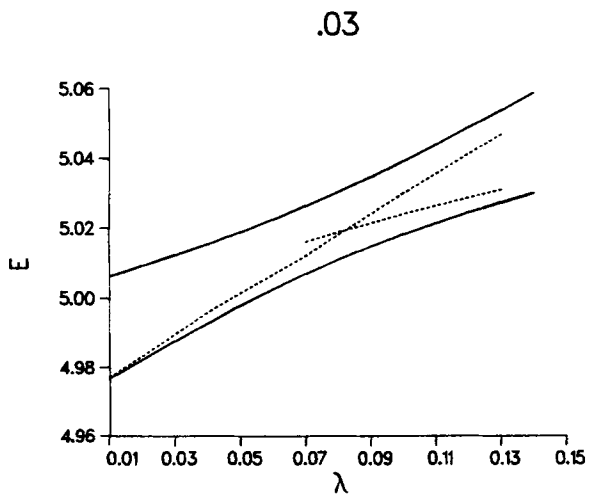

FIG. 3. Same as Fig. 1 but with $b = 0.03$. Semiclassical eigenvalues of Table II are indicated with a dotted line.

the λ at the avoided crossing are given in Fig. 5. One sees the expected mixing of the two nodal patterns in the latter.

We turn next to a comparison with a perturbation treatment of the splitting in the avoided intersection region. Quantum mechanically the energies in Figs. 1–3 are of the approximate form[5]

$$E_{\pm} \simeq \tfrac{1}{2}(H_{11} + H_{22}) \pm \tfrac{1}{2}\left[4|H_{12}|^2 + (H_{11} - H_{22})^2\right]^{1/2} , \qquad (2)$$

so that at the avoided intersection ($H_{11} = H_{22}$), the splitting is $2|H_{12}|$. H_{12} calculated by perturbation theory using harmonic oscillator (0, 3) and (1, 0) wave functions is given by $\int \psi_{03}^0 H \psi_{10}^0 \, dx\, dy$. Only the xy^3 term in Eq. (1) contributes to this H_{12}. For a state (n_x, n_y) denoted by $(v_x, v_x - 1)$ interacting with a state $(v_y - 3, v_y)$ the matrix element is found to be

$$H_{12} = -\left[v_x v_y (v_y - 1)(v_y - 2)/\omega_x^0 \omega_y^{03}\right]^{\frac{1}{2}} b/4 . \qquad (3)$$

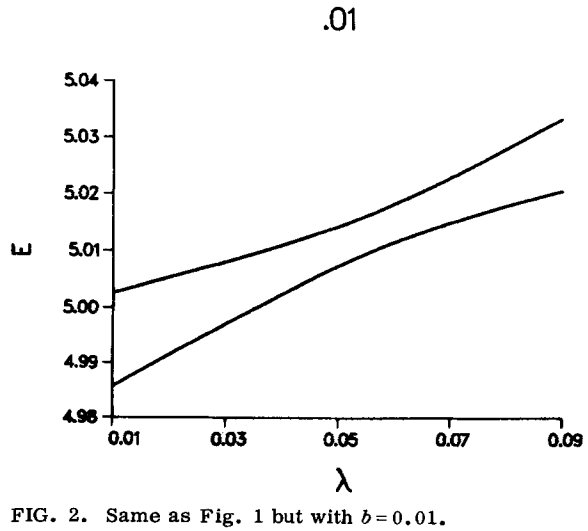

FIG. 2. Same as Fig. 1 but with $b = 0.01$.

In the particular case of the (1, 0) and (0, 3) states one has

$$H_{12} = -\left[6/\omega_x^0 \omega_y^{03}\right]^{1/2} b/4 . \qquad (4)$$

The results of Eq. (4) for the splitting are given in Table I, where they are compared with the exact quantum mechanical results. They agree quite well. $H_{11}(\lambda)$ and $H_{22}(\lambda)$ could also be computed, including now the x^3, y^3 and x^2y^2 terms, but for reasons discussed later we are particularly interested in H_{12} at the avoided intersection.

Classical and semiclassical calculation

We consider next the classical behavior. Trajectories were obtained by integrating the equations of motion for the Hamiltonian (1.1) using the DEROOT program.[6] A typical trajectory is shown in Fig. 6. One half-cycle of the trajectory is seen to be S shaped (reflecting the fact that $\omega_x^0 = 3\omega_y^0$), i.e., there are three half-cycles of the x motion to one of the y. To quantize this trajectory we use methods described previously[7,8]: The Poincaré surface of section results are recorded for p_y vs y each time the trajectory crosses the line x = constant (in the present case we used $x = 0$) in a particular direction (e.g., $\dot{x} > 0$). Originally we plotted p_y vs y at $x = 0$ and calculated the area $\oint p_y dy$.[7] Subsequently, we found[8] that evaluation of this area via an action-angle plot (J_y^0 vs w_y^0) required fewer trajectory points (shorter time trajectory) since J_y^0 is much more nearly constant than p_y. Thus, instead, we evaluate the $\oint J_y^0 dw_y^0$ area. J_y^0 and w_y^0 variables are deduced from y and p_y via the usual harmonic oscillator expressions[9]:

$$2\pi w_y^0 = \tan^{-1}(\omega_y^0 y/p_y) , \quad J_y^0 = \pi(p_y^2 + \omega_y^{02} y^2)/\omega_y^0 , \qquad (5)$$

with a standard convention on the relation between the phase of w_y^0 and the sign of p_y. Similarly for $y = 0$ the area $\oint J_x^0 dw_x^0$ was calculated. These integrals are set equal to $(n_y + \frac{1}{2})h$ and $(n_x + \frac{1}{2})h$, respectively, and the initial conditions of the trajectory are varied until the

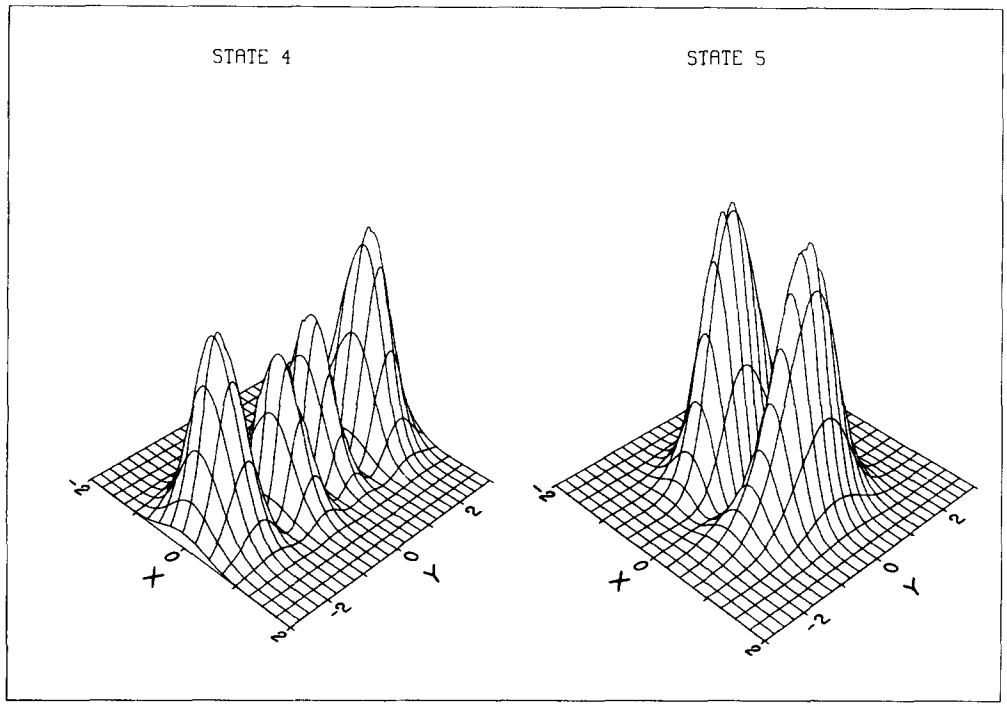

FIG. 4. Plot of the square of wave functions for Fig. 1 at $\lambda = 0.01$.

n_x and n_y are the desired integers. As a check we also calculated the phase integral $\int(p_x dx + p_y dy)$ along the cycle of the trajectory and joined the ends on the $y = 0$ surface of section [the trajectory close method of Ref. 7(c)]. This integral and the $\oint J_x^0 dx^0$ integral served to determine the eigentrajectory. The two methods agreed to ± 0.0005.

A comparison of quantal and semiclassical eigenvalues for the (0, 3) and (1, 0) states are given in Table II and Figs. 1 and 3 for $b = 0.005$ and 0.03. In following the behavior of the energy of each semiclassical state (0, 3) and (1, 0), we observed that it passes through the region of the avoided crossing instead of showing an energy level repulsion there. The present semiclassical method ("primitive semiclassical", i.e., no uniform approximation) does not yield the splitting and so in the vicinity of the avoided crossing the comparison (indicated by footnote a in Table II) is made with the mean of quantum eigenvalues for (0, 3) and (1, 0) states. This limitation

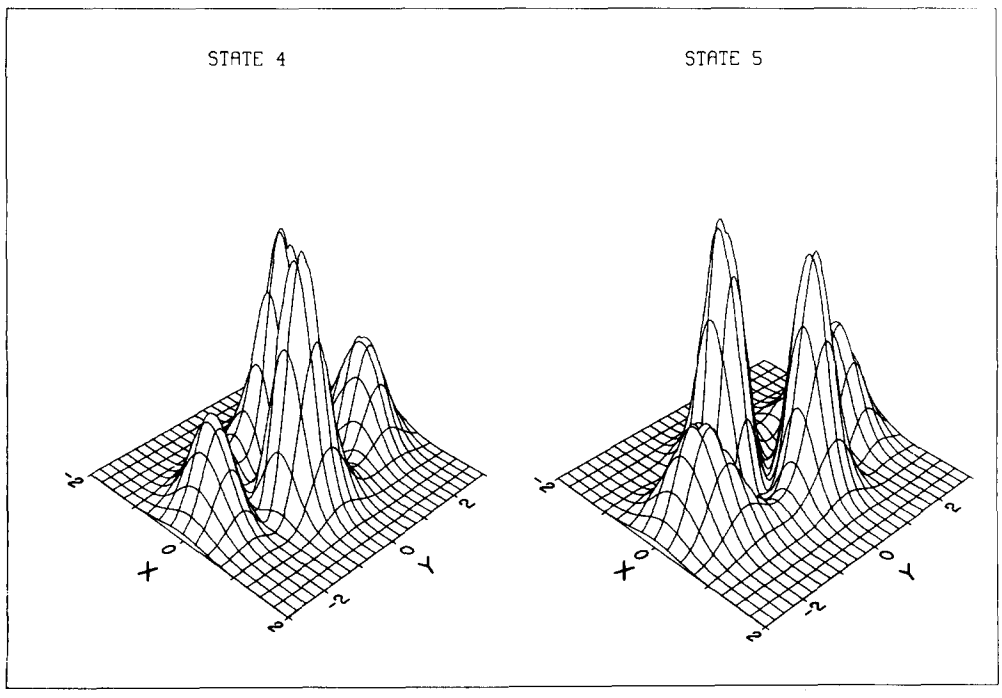

FIG. 5. Plot of the square of the wave function for Fig. 1 at the avoided intersection ($\lambda = 0.055$).

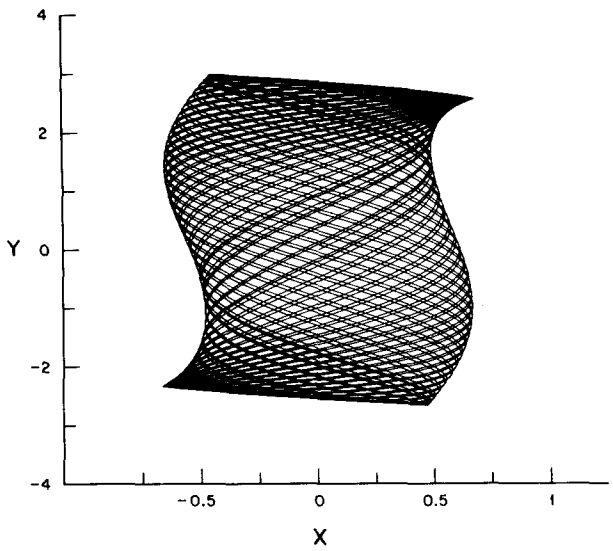

FIG. 6. Plot of the classical trajectory ("eigentrajectory") which corresponds semiclassically to the (0, 3) state at $b = 0.005$, $\lambda = 0.01$, i.e., to the left $|\psi|^2$ in Fig. 4.

TABLE II. Comparison of quantum and semiclassical eigenvalues for the (0, 3) and (1, 0) states.

b	λ	E_Q (0, 3)	E_{SC} (0, 3)	E_Q (1, 0)	E_{SC} (1, 0)
0.005	0.01	4.987	4.987	5.002	...[b]
	0.03	4.998	4.999	5.007	5.007
	0.05	5.011[a]	5.010	5.011[a]	5.012
	0.055	5.013[a]	5.013	5.013[a]	5.013
	0.060	5.015[a]	5.016	5.015[a]	5.014
	0.080	5.028	5.027	5.019	5.019
0.03	0.01	4.977	4.977	5.006	...[c]
	0.04	4.993	4.996	5.015	...[d]
	0.07	5.017[a]	5.012	5.017[a]	5.016
	0.10	5.029[a]	5.030	5.029[a]	5.024
	0.13	5.054	5.047	5.027	5.031

[a]The five values labeled a in this column are averages of the following respective pairs: (5.0092, 5.0128), (5.0114, 5.0147), (5.0132, 5.0169), (5.0069, 5.0262), (5.0181, 5.0392).
[b]Smallest $J_x \sim 3.12\pi$ instead of $J_x = 3\pi$.
[c]Smallest $J_x \sim 3.18\pi$ instead of $J_x = 3\pi$.
[d]Smallest $J_x \sim 3.11\pi$ instead of $J_x = 3\pi$.

can be avoided, as discussed later.

At $b = 0.03$, a new type of trajectory was readily found (Fig. 7). It was obtained using action variables (J_x^0, J_y^0) which were approximately the mean of those for the (0, 3) and (1, 0) states, i.e., $J_x^0 = \frac{1}{2}(0 + \frac{1}{2} + 1 + \frac{1}{2})h$ and $J_y = \frac{1}{2}(3 + \frac{1}{2} + 0 + \frac{1}{2})h$. After some iteration a trajectory was found whose p_x vs x Poincaré surface of section plot at $y = 0$ showed two ovals connected near the lower part of the figure (Fig. 8). The inner oval had an area of about 1.25π and the larger oval had an area of about 2.88π. The corresponding J_x^0 vs w_x^0 surface of the section is plotted in Fig. 9. The time dependence of the J^0's shows a cusplike oscillation between the J^0's roughly of the (0, 3) state and of the (1, 0) state; as in Fig. 10 for J_x^0.

The plot in Fig. 8 is actually the separatrix or nearly the separatrix for two different types of motion. In the first of these the p_x vs x plot is a closed curve lying entirely within the small oval in Fig. 8, and at the appropriate energy one such curve corresponds to the (0, 3) state. The shape of the trajectory is more or less elongated boxlike. In the second type of motion, produced by another set of initial conditions at any energy, the p_x vs x plot is a closed curve lying between the two ovals and is somewhat half-moon shaped and exhibit S shaped trajectories. Outside the larger oval in Fig. 8, a px vs x plot is a closed curve and at the appropriate energy one such curve corresponds to the (1, 0) state.

We consider next a semiclassical estimate of the splitting in the intersection region, a splitting not obtained in the primitive semiclassical results. We make use of Eq. (2). To calculate H_{12} we introduce the semiclassical basis set wave functions in terms of angle variables w_x and w_y for the mean motion at the intersection, and use a simple semiclassical perturbation theory.

TABLE I. Splitting of energy levels at the intersection.[a,b]

b	Quantum	Quantum perturbation	Semiclassical perturbation
0.005	0.0033	0.0035	0.0041
0.01	0.0066	0.0070	0.0082
0.03	0.0193	0.0210	0.0246

[a]Defined as the minimum value of $|E_1 - E_2|$, using $\Delta\lambda$ increments given in the text.
[b]2 $|H_{12}|$ calculated, respectively, from 100-harmonic oscillator quantum mechanical basis set, quantum [Eq. (4)] and semiclassical [Eq. (8)] perturbation formulas.

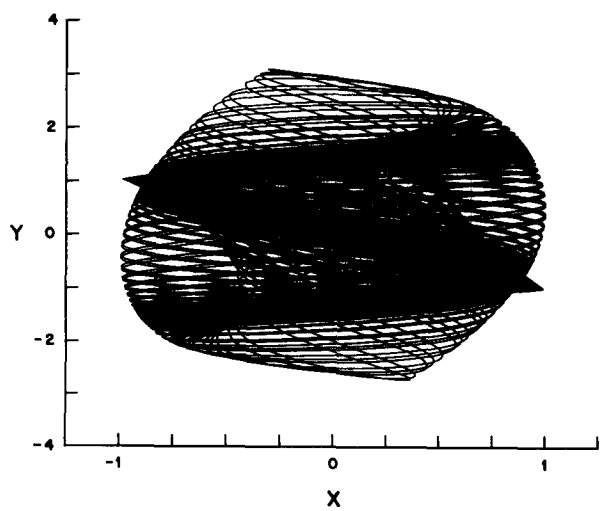

FIG. 7. A transition-type trajectory for $b = 0.03$, $\lambda = 0.070$, $E = 5.01$.

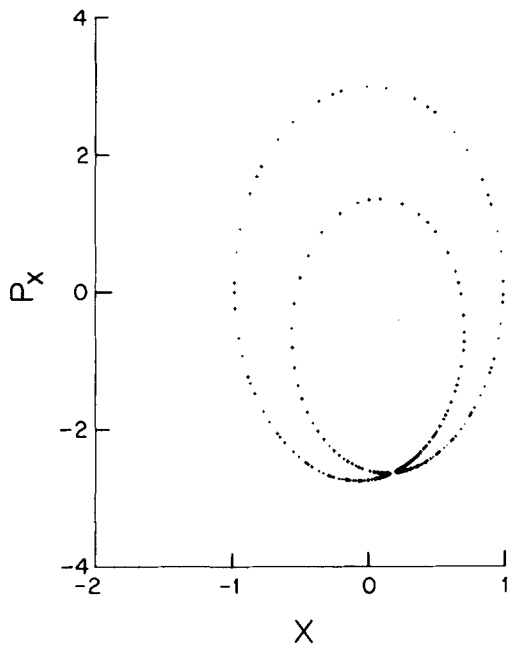

FIG. 8. Plot of p_x vs x at $(y=0, \dot{y}>0)$ for the trajectory in Fig. 7.

The lowest order perturbation theory is one where the semiclassical basis set ψ^0 involves angle variables w_x^0 and w_y^0 for the harmonic oscillator problem. We then have

$$H_{12} \simeq \iint \psi_{03}^{0*}(w_x^0, w_y^0) H \psi_{01}^0(w_x^0, w_y^0)\, dw_x^0\, dw_y^0 ,$$

$$\psi^0 = \exp 2\pi i(n_x w_x^0 + n_y w_y^0) , \qquad (6)$$

where the integrals are over a unit interval, and (n_x, n_y) equals (0, 3) and (1, 0) for ψ_{03}^0 and ψ_{10}^0, respectively. The only term in H in Eq. (1) which makes a contribution to this integral is the resonant coupling term $-bxy^3$. This xy^3 is next expressed in terms of the unperturbed action-angle variables. For the J_x^0 and J_y^0 appearing in this xy^3 the mean of those in the two states is used, as in Ref. 10 where the spectral matrix elements were calculated with mean J^0's, for reasons given there.

One finds that

$$H_{12} = -(J_x^0 J_y^{03}/\omega_x^0 \omega_y^{03})^{1/2}\, b/4(2\pi)^2 , \qquad (7)$$

where J_x^0 and J_y^0 have mean values $\frac{1}{2}(\frac{1}{2}+1\frac{1}{2})h$ and $\frac{1}{2}(3\frac{1}{2}+\frac{1}{2})h$, respectively, and $\omega_x = 3\omega_y = 3$. In the limit where the fractional difference of the J_x^0's in the two states is small and similarly for the J_y^0's, Eq. (7) is seen to approach Eq. (3), as indeed it should by the correspondence principle. (We note that $J/2\pi = v + \frac{1}{2}$.) The case where there should be the greatest discrepancy between the two equations is the present one, namely the matrix element of the (1, 0) and (0, 3) states. For these states one finds

$$H_{12} = -(8/\omega_x^0 \omega_y^{03})^{1/2}\, b/4 . \qquad (8)$$

The difference between Eqs. (4) and (8) is only approximately 15% for this worst case. The results for $2|H_{12}|$ are given in Table I.

An improved value of H_{12}, but still limited by the mean action approximation, should be one where the w^0's in Eq. (6) are replaced by more exact w's. A mean action trajectory, generated from a Hamiltonian with xy^3 absent, was used to calculate the spectrum of xy^3. From the intensity near the origin, and the spectral theory described in the Appendix, $2|H_{12}|$ was estimated to be $0.8b$, which is comparable to the values in Table I. This estimate of a low intensity line at very low frequency (which was $\omega = 0.0024$ in the present case) required 2^{17} points for the Fourier transformation, with a corresponding frequency resolution of 2×10^{-4}.

DISCUSSION

We have seen that the primitive semiclassical method yields eigenvalue curves which pass through the avoided crossing rather than undergoing a level repulsion, but which otherwise yields good agreement with the quantum eigenvalues (Table II).

For the present system the (1, 0) and (0, 3) classical states appear to be distinct. (We found the isolated states in most cases.) Thus, they are connected to each other in the avoided crossing region by a quantum mechanical tunneling process. Such a tunneling occurs, e.g., between the librating trajectories in the Henon–Heiles potential,[11] in compound state resonances in another system,[12] as well as in others. The barrier for the trajectory in these cases is not a potential energy one but rather one imposed by the constants of the motion (the action variables),[13] much as a centrifugal barrier arises from an action variable, the angular momentum, and an attractive force.

When the coupling term causing the "tunneling" can be identified, as in the present case, the splitting of the crossed levels can be estimated from the perturbation theory, as in Table I. Classical canonical perturbation theory[14] and semiclassical uniform approximations[15,16] have been used to treat other semiclassical eigenvalue problems, and we have adapted them to the present problem.[17] Results based on a perturbation approxima-

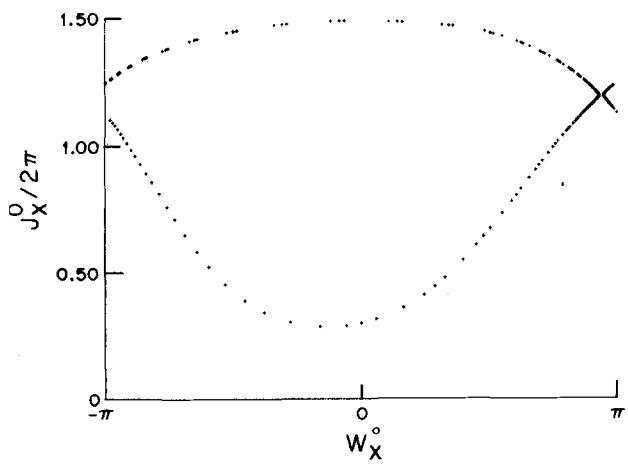

FIG. 9. Surface of section plot of J_x^0 vs w_x^0 for the trajectory in Fig. 7.

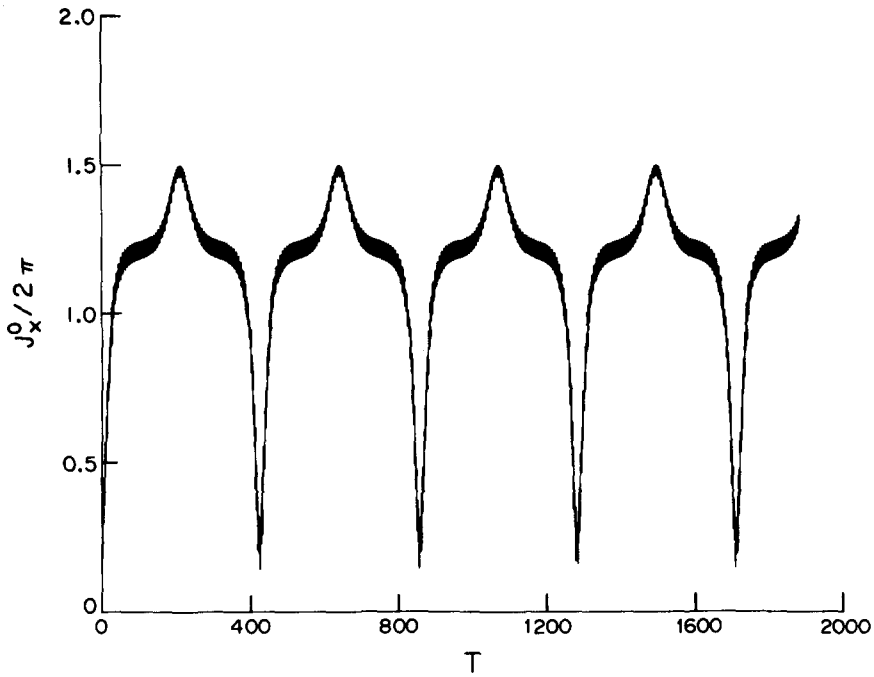

FIG. 10. Plot of J_x^0 vs time for the trajectory in Fig. 7.

tion have been obtained,[17] and are consistent with the repulsion of the levels displayed in Figs. 1–3.

The trajectory in Figs. 7–10, which undergoes a transition between the two zeroth order states in a regular (quasiperiodic) manner, is at or near the "separatrix," and is narrower, i.e., more difficult to find, at low b's than at high. (The "resonance width" is smaller at small b's, being proportional to $b^{1/2}$ by Chirikov's theory.[18]) The oscillation between the two states is similar to one which we found in a study of the Fermi resonance system,[19] to one found in the laser-driven Morse oscillator problem,[20] and is related to but not the same as the apparently more random flipping found by Reinhardt and co-workers between librating and precessing trajectories in the Henon–Heiles system.[14]

As suggested earlier[2] a classical resonance leads to an avoided crossing. One sees both quantum mechanically and classically that this resonance facilates the distribution of excitation among different modes, e.g., between the different zeroth order states in Figs. 4 and 6, as in Figs. 5 and 7. Interestingly enough, the results show that the classical state is (in the vicinity of an avoided crossing) less delocalized than the quantum state, apart from trajectories near the separatrix trajectory. Thus, in the classically quasiperiodic regime some classical trajectories may predict less energy randomization than the quantum treatment, because of the absence of tunneling. In the classically chaotic regime the reverse can be true: The system may appear as classically chaotic but the density of states may be too small to cause irregularities in the spectrum or in the nodal patterns of the wave functions. functions.[1–3]

ACKNOWLEDGMENTS

We are pleased to acknowledge the support of the present research by the U.S. Department of Energy under contract W-7405-eng-26 with the Union Carbide Corporation (at Oak Ridge) and by a grant from the National Science Foundation (at the California Institute of Technology).

APPENDIX: FOURIER TRANSFORM CALCULATION OF H_{12}

A formula which should be an improvement over Eq. (6) would entail using the latter but with a more exact choice of action-angle variables (J, w) generated, e.g., by a trajectory arising from the H in Eq. (1) with only the $-bxy^3$ removed. The only term in H which contributes to the integral for H_{12} is now $-bxy^3$. The semiclassical wave functions are those given in Eq. (6), but with the w^0's replaced by the w's for this trajectory. One sees from this new Eq. (6) that we need to calculate a Fourier component $(n_x^2 - n_x^1)$, $(n_y^2 - n_y^1)$ of $-bxy^3$. In our case this will be the (1–0), (0–3) component, i.e., the $(\omega_x - 3\omega_y)$ component, where the ω's denote the exact frequencies of the new Hamiltonian $H + bxy^3$, rather than the ω^0's in Eq. (1). We first note that when the dynamical motion is quasiperiodic, any dynamical function $f(t)$, $-bxy^3$, e.g., can be expanded in a Fourier series in the exact angle variables $(w_1, \ldots, w_N)$ for this N-coordinate system:

$$f(t) = \sum_m f_m \left(\exp \sum_{i=1}^{N} 2\pi i m_i w_i \right) , \tag{A1}$$

where f_m denotes $f_{m_1,\ldots,m_N}$. The characteristic angular frequencies for each w_i are ω_i ($2\pi w_i = \omega_i t + \phi_i$, where ϕ_i is an initial phase). In our case H_{12} equals the f_m corresponding to $m_x = 1$ and $m_y = -3$. The f_m's can be calculated as in our spectral analysis[10,11]: The Fourier transform $I(\omega)$ of the autocorrelation function $f(0)f(t)$ is considered:

$$I(\omega) = \frac{1}{2\pi} \int_{-\infty}^{\infty} f(0) f(t) \exp(-i\omega t)\, dt . \tag{A2}$$

This $I(\omega)$ is related to the following time average, as before[11]:

$$I(\omega) = \frac{1}{2\pi} \lim_{T\to\infty} \frac{1}{T} \left| \int_0^T f(t) \exp(-i\omega t)\, dt \right|^2 . \qquad \text{(A3)}$$

(The two expressions differ by a term which vanishes as $T \to \infty$.) When the expansion (A1) is introduced into Eq. (A3) one finds

$$I(\omega) = \sum_m |f_m|^2 \delta \left(\sum_{i=1}^N m_i \omega_i - \omega \right) . \qquad \text{(A4)}$$

Thus, the desired quantity $|f_m|$ is the square root of the coefficient of the relevant dirac delta function in Eq. (A4). Each spectral line approaches a delta function as $T \to \infty$, but for finite T the integrated area of $I(\omega)$ vs ω in the vicinity of the line gives $|f_m|^2$. The height of the line is proportional to T and the width is inversely proportional. Thus, when one calculates the height of the peak and divides by T one obtains a quantity independent of the trajectory time and proportional to the area. Since heights are easier to measure than areas we have used this indirect way of evaluating the area.[10,11] The relation between area and height was obtained via a suitable test function.

For $f(t)$ we have used $-bxy^3$ and looked at the intensity of the appropriate Fourier component $\Sigma m_i \omega_i$ band, namely $\omega_x - 3\omega_y$. The Fourier transform of the mean action trajectory near the avoided crossing was calculated, and the results for the splitting obtained in this way are given in the text.

[1]D. W. Noid, M. L. Koszykowski, and R. A. Marcus, Annu. Rev. Phys. Chem. **32**, 267 (1981), and references cited therein.

[2]R. A. Marcus, in *Horizons of Quantum Chemistry*, edited by K. Fukui and B. Pullman (Reidel, Dordrecht, 1980), p. 107; D. W. Noid, M. L. Koszykowski, and R. A. Marcus, Chem. Phys. Lett. **73**, 269 (1980); D. W. Noid, M. L. Koszykowski, M. Tabor, and R. A. Marcus, J. Chem. Phys. **72**, 6169 (1980); R. Ramaswamy and R. A. Marcus, *ibid.* **74**, 1379 (1981).

[3]R. A. Marcus, Ann. N. Y. Acad. Sci. **357**, 169 (1980).

[4]Developed by National Activity to Test Software, *Lecture Notes in Computer Science*, edited by G. Goos and J. Hartman (Springer, Berlin, 1976), Vol. 6.

[5]A. S. Davydov, *Quantum Mechanics* (Pergamon, New York, 1965), p. 176.

[6]L. F. Shampine and M. K. Gordon, *Computer Solution of Ordinary Differential Equations: The Initial Value Program* (Freeman, San Francisco, 1975).

[7](a) D. W. Noid and R. A. Marcus, J. Chem. Phys. **62**, 2119 (1975); W. Eastes and R. A. Marcus, *ibid.* **61**, 4301 (1974); (b) D. W. Noid and R. A. Marcus, *ibid.* **67**, 559 (1977); (c) D. W. Noid, M. L. Koszykowski, and R. A. Marcus, *ibid.* **71**, 2964 (1979).

[8]D. W. Noid, M. L. Koszykowski, and R. A. Marcus, J. Chem. Phys. **73**, 391 (1980).

[9]M. Born, *Mechanics of the Atom* (Ungar, New York, 1960).

[10]M. L. Koszykowski, D. W. Noid, and R. A. Marcus, J. Phys. Chem. **86**, 2113 (1982).

[11]D. W. Noid, M. L. Koszykowski, and R. A. Marcus, J. Chem. Phys. **67**, 404 (1977).

[12]D. W. Noid and M. L. Koszykowski, Chem. Phys. Lett. **73**, 114 (1980).

[13]A term coined for this is dynamic tunneling: M. J. Davis and E. J. Heller, J. Chem. Phys. **75**, 246 (1981).

[14]Work of Percival, Delos, Miller, Reinhardt, Handy, Schatz, and others, cited in Ref. 1; J. A. Sanders, J. Chem. Phys. **74**, 5733 (1981).

[15]J. N. L. Connor, Chem. Phys. Lett. **4**, 419 (1969), for the semiclassical uniform approximation for a double well potential.

[16]See W. P. Reinhardt, J. Phys. Chem. **86**, 2158 (1982), and references cited therein.

[17]T. Uzer, D. W. Noid, and R. A. Marcus (to be submitted).

[18]G. M. Zaslavskii and B. V. Chirikov, Sov. Phys. Usp. **14**, 549 (1972); B. V. Chirikov, Phys. Rep. **52**, 263 (1979), and references cited therein.

[19]D. W. Noid, Ph.D. thesis, University of Illinois, 1976, Fig. 18.

[20]J. R. Stine and D. W. Noid (to be published).